11-2023

Chapter 4.1: Visualizing the Solubility of Salts Via 3-D Topo Surfaces: Pyramids with Ridges and Plateaus

Garon C. Smith

Md Mainul Hossain

Chapter 4.1
Visualizing the Solubility of Salts Via 3-D Topo Surfaces: Pyramids with Ridges and Plateaus

Garon C. Smith[1] and Md Mainul Hossain[2]
[1]Department of Chemistry and Biochemistry, University of Montana, Missoula, MT 59812, USA
[2]Department of Biochemistry and Microbiology, North South University, Dhaka 1229, Bangladesh

Abstract
A new 3-D graphical representation for the solubility of sparingly soluble salts in aqueous solutions has been developed utilizing a new composition grid. In this case, the x-axis carries the concentration of the salt's cation (usually a metal) and the y-axis holds the concentration of the salt's anion. Plotted above the grid are a salt's solubility, individual species concentrations or distribution coefficients. Three levels of sophistication in the descriptive chemistry are discussed. In Case 1, the only dissolved species included are the cation and anion present in the salt's solubility product expression, the $\mathcal{K}_{sp}$. Case 2 adds the possibility of ion pairs or neutral complexes. Finally, Case 3 encompasses all complexes for which thermodynamic constants are available. Example systems include the 1:1 AgCl and the 1:2 PbI_2 salts. The composition grid approach addresses not only the solubility of a solid salt in pure water, but essentially all other feasible conditions in which one or the other of the component ions is present in the dissolving liquid phase. Case 1 gives rise to 3-D solubility surfaces (topos) that have a pyramidal shape. Case 2 possesses plateaus under saturated conditions where the concentration of the ion pair or neutral complex dominates. Case 3 can add extra ramps under saturated conditions when other complexes become important. A comparison of the topos from all three cases for a given salt allows the user to see the effects of incompletely capturing the possible chemical processes that contribute to solubility. In the AgCl system, for example, the Case 3 maximum solubility was 12.5 times greater than that predicted for Case 1. Included as supplementary files for the chapter are the downloadable Solubility TOPOS software (an Excel workbook), a PowerPoint lecture, teaching materials, a detailed description of the formulas and algorithms used to solve for solubility, and a Visual Basic code listing.

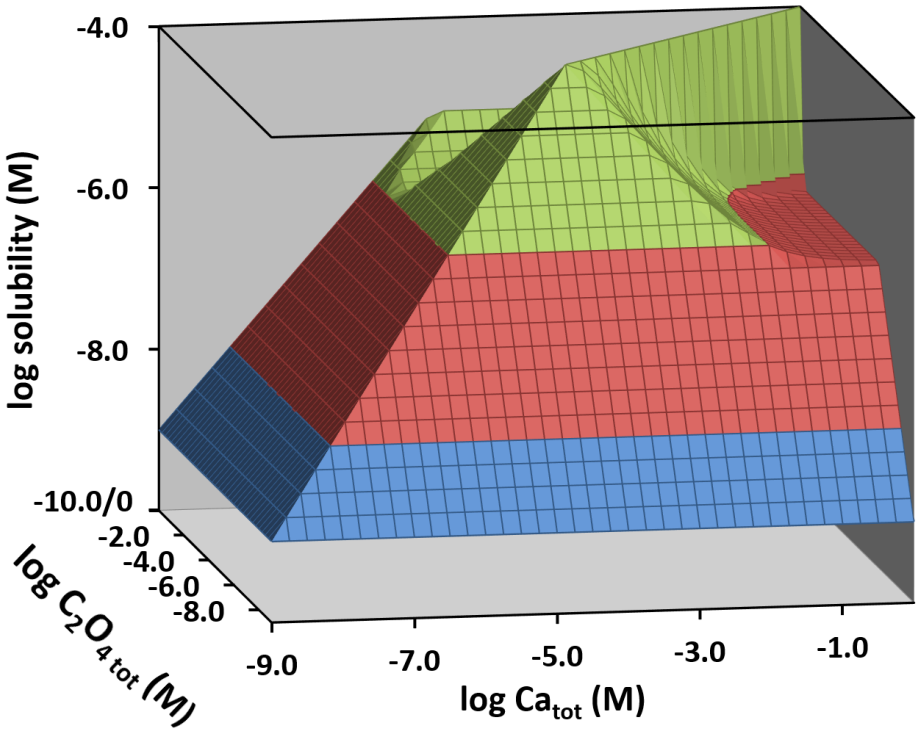

4.1.1 Introduction

When the equilibrium behavior of slightly soluble salts is introduced in introductory chemistry courses, it is traditionally taught from the standpoint of the simple solubility product, or $\mathcal{K}_{sp}$, that is associated with its dissolution reaction.[1] If one ignores charges for the moment, a metal salt with an anionic ligand can be represented as M_mL_n. The general dissolution reaction would be

$$M_mL_n \rightleftharpoons m\,M + n\,L \qquad (4.1\text{-}1)$$

and its solubility product expression would be

$$\mathcal{K}_{sp} = [M]^m[L]^n \qquad (4.1\text{-}2)$$

where *m* and *n* are the stochiometric ratios of the salt's empirical formula. (This same notation also holds for other cations such as NH_4^+ and quaternary amine species.) The solubility product expression, $\mathcal{K}_{sp}$, was first introduced by Walther Nernst in 1889.[2]

Using just the $\mathcal{K}_{sp}$ to characterize solubility is usually an inadequate description of the rich chemistry that can occur in solution.[1] Ion pairing, dissolved aqueous complexes, hydrolysis reactions, and polynuclear species are all possibilities. Figure 4.1-1, for example, illustrates possible additional processes that could occur in the AgCl system. 3-D visualization of solubility topo surfaces above a cation-anion composition grid can systematically address each of these complicating side-reactions and reveal the conditions under which they become significant. This chapter illustrates how inadequate a $\mathcal{K}_{sp}$-only model is in describing solubility of an ionic solid. The additional side reactions can significantly enhance the solubility limits of a salt.

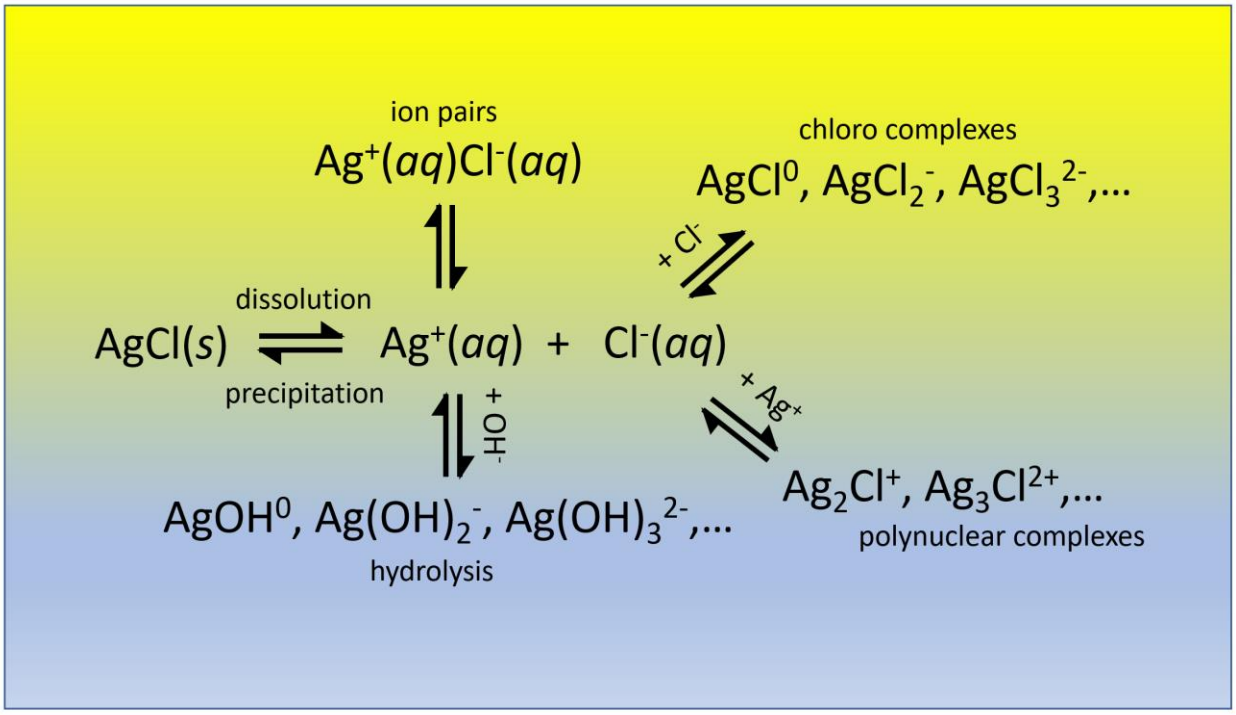

Figure 4.1-1. Some possible interactions in the AgCl system.

4.1.2 The Solubility Composition Grid

The composition grid for solubility topo surfaces (Figure 4.1-2) shows the total analytical concentration of the anion (usually a ligand), L_{tot}, on the y-axis and the total analytical concentration of the cation (usually a metal ion) on the x-axis, M_{tot}. In order to cover a wide range of possible conditions and phenomena, both axes are shown here in their logarithmic mode. Concentrations run from trace

levels, 10^{-9} M, to rather concentrated conditions, 10^{0} = 1 M. If increments along the axes are set at 0.25 log units, the overall grid encompasses 37 points by 37 points for a total of 1369 points. Thus, an equilibrium calculation must be completed for each of these points in generating a solubility surface.

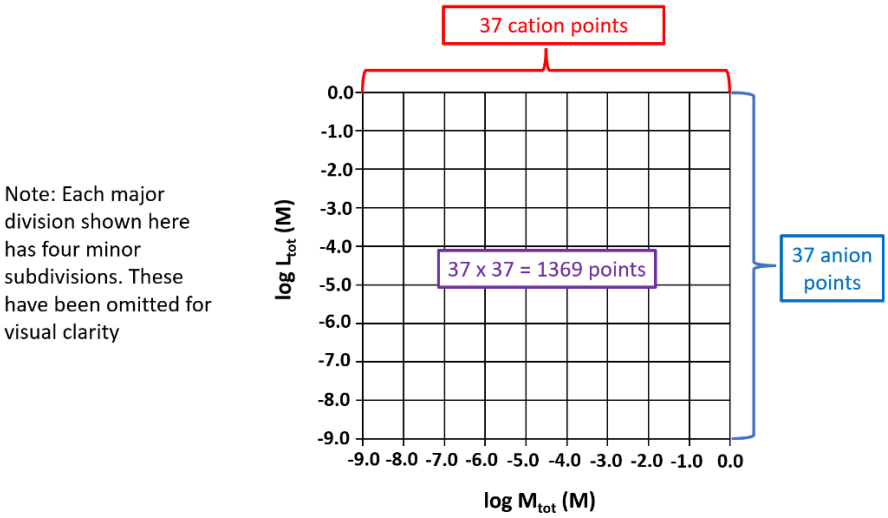

Figure 4.1-2. The solubility composition grid.

The primary *z*-axis for solubility surfaces will represent the overall concentration of the dissolved salt of interest, often in the presence of common ions. The compositions for the surface include more than just adding a solid ionic salt to water. A broader view of solubility must be kept in mind. Consider, for example, the AgCl system of Figure 4.1-1. Adding successive amounts of AgCl to pure water corresponds to the limited set of 37 grid points that define a diagonal trace across the composition grid from the lower left corner of the grid to the upper right. They are compositions which have the perfect 1:1 ratio of Ag^+ to Cl^-. Not only can these points represent adding solid AgCl to pure water, they could equivalently be a situation in which an Ag^+-containing solution and a Cl^--containing solution are mixed in an exact stoichiometric ratio. The other 1332 grid points are not included yet. These off-diagonal points represent mixtures in which either Ag^+ or Cl^- is in excess. This broader investigation of the AgCl system can be visualized as mixing various combinations of Ag^+ and Cl^- solutions to possibly produce some solid precipitate. When the two solutions are mixed in non-stoichiometric ratios, an off-diagonal point will be encountered.

The definition of solubility shifts from one region of the topo surface to another to take into account those situations in which common ions are present. Without common ions, *i.e.*, a stoichiometric mix, the solubility of the salt can be

determined from either of its component ions. With common ions around, however, their influence on solubility equilibrium must be taken into account. In the simple $\mathcal{K}_{sp}$-only case for AgCl, just a 1:1 salt exists. Under excess Cl^- conditions, the solubility will be defined by the $[Ag^+]$ concentration. The only way that Ag^+ is present in the solution phase is from the dissolved, unprecipitated Ag^+. In excess Cl, the Cl^- is mostly from the preexisting Cl^--containing solution. Likewise, under excess Ag^+ conditions, it is the $[Cl^-]$ that finds its way into solution that determines the solubility. These are summarized in Table 4.1-1.

Table 4.1-1. Solubility definitions for AgCl solubility in a $\mathcal{K}_{sp}$-only case

Composition grid region	Solubility definition
Stoichiometric mix diagonal	$[Ag^+]$ or $[Cl^-]$
In excess Cl	$[Ag^+]$
In excess Ag	$[Cl^-]$

4.1.3 Solubility Topo Surfaces for a $\mathcal{K}_{sp}$-only Case

A downloadable Microsoft Excel workbook, Solubility TOPOS, has been created with embedded Visual Basic macros to automatically compute and plot the solubility topos. For $\mathcal{K}_{sp}$-only systems, the only required inputs are the designation of a salt's stoichiometry and the associated $\mathcal{K}_{sp}$ value. For illustrative purposes, we continue with the AgCl system. It was chosen because it has been extensively studied; there is a large body of available thermodynamic and experimental data. For the simple $\mathcal{K}_{sp}$-only model, a value of 1.8×10^{-10} was adopted.[3] In order to calculate the complete solubility topo surface, six different solubility computational procedures were employed depending on the region of the composition grid (Figure 4.1-3).

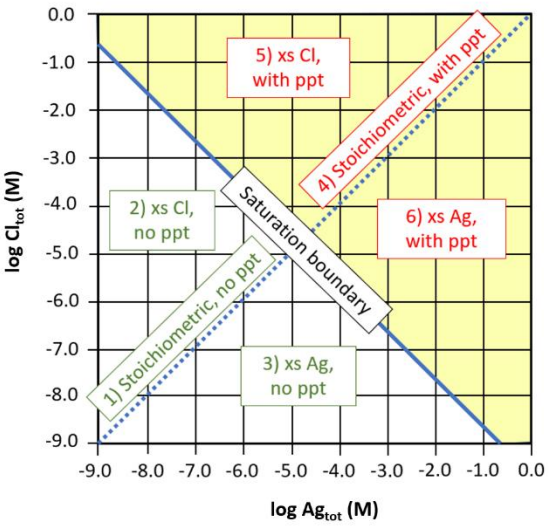

Figure 4.1-3. Solubility assignment regions for the AgCl system.

Three regions of Figure 4.1-3, numbered 1 through 3, are associated with unsaturated solutions. Three others, numbered 4 through 6, correspond to saturated conditions. Separating the two groups of regions is the diagonal saturation boundary that is determined explicitly by the $\mathcal{K}_{sp}$ value. Because the saturation boundary intersects the left and bottom edges of the grid, one or the other component is at 1.0×10^{-9} M. The saturation boundary, as shown below, intersects each axis at log 1.8×10^{-1} or -0.74.

$$\left[Ag^+\right] \text{or} \left[Cl^-\right] = \frac{\mathcal{K}_{sp}}{1 \times 10^{-9}} = \frac{1.8 \times 10^{-10}}{1 \times 10^{-9}} = 1.8 \times 10^{-1} \text{M} \qquad (4.1\text{-}3)$$

For Regions 1 through 3, no solid AgCl is present. For the stoichiometric mix of Region 1, either log $[Ag^+]$ or $[Cl^-]$ provides the solubility value. Region 2 contains all compositions where AgCl completely dissolves in excess Cl conditions. Since there is more Cl^- than could be associated with AgCl that dissolved, we define the amount of dissolved AgCl as the $[Ag^+]$ value. The complementary case occurs over Region 3 where there is excess Ag. Here the solubility will be determined as $[Cl^-]$. These assignments generate two sections on the grid that meet at the Region 1 stoichiometric mix line.

Regions 4 through 6 are analogous to Regions 1 through 3 except that some solid AgCl is present as a precipitate. Region 4 is the stoichiometric mix line while Regions 5 and 6 have excess Cl or Ag, respectively. The solubility definitions remain the same, but the calculations must include the $\mathcal{K}_{sp}$ equation as an extra equilibrium constraint that accounts for the quantity of precipitate.

Once the stoichiometry and $\mathcal{K}_{sp}$ value for an ionic solid have been entered into the Solubility TOPOS and embedded macros run, the results are presented as a pair of 3-D topo surfaces – a wire-frame version and a contour map version. The wire-frame (Figure 4.1-4a) is presented as a color-filled topo because the pyramidal surface structure is difficult to perceive in an open wire-frame plot. We have, however, superimposed the grid on the surface so that the coordinate system can be seen. Because of the viewing angle, only half of the wire-frame surface is visible. In this instance, a 1:1 stoichiometry, the surface is symmetric with respect to the stoichiometric mix line, so both halves will be identical in appearance. The contour map version (Figure 4.1-4b) makes it easy to read the (x,y) grid coordinates at any point of the grid.

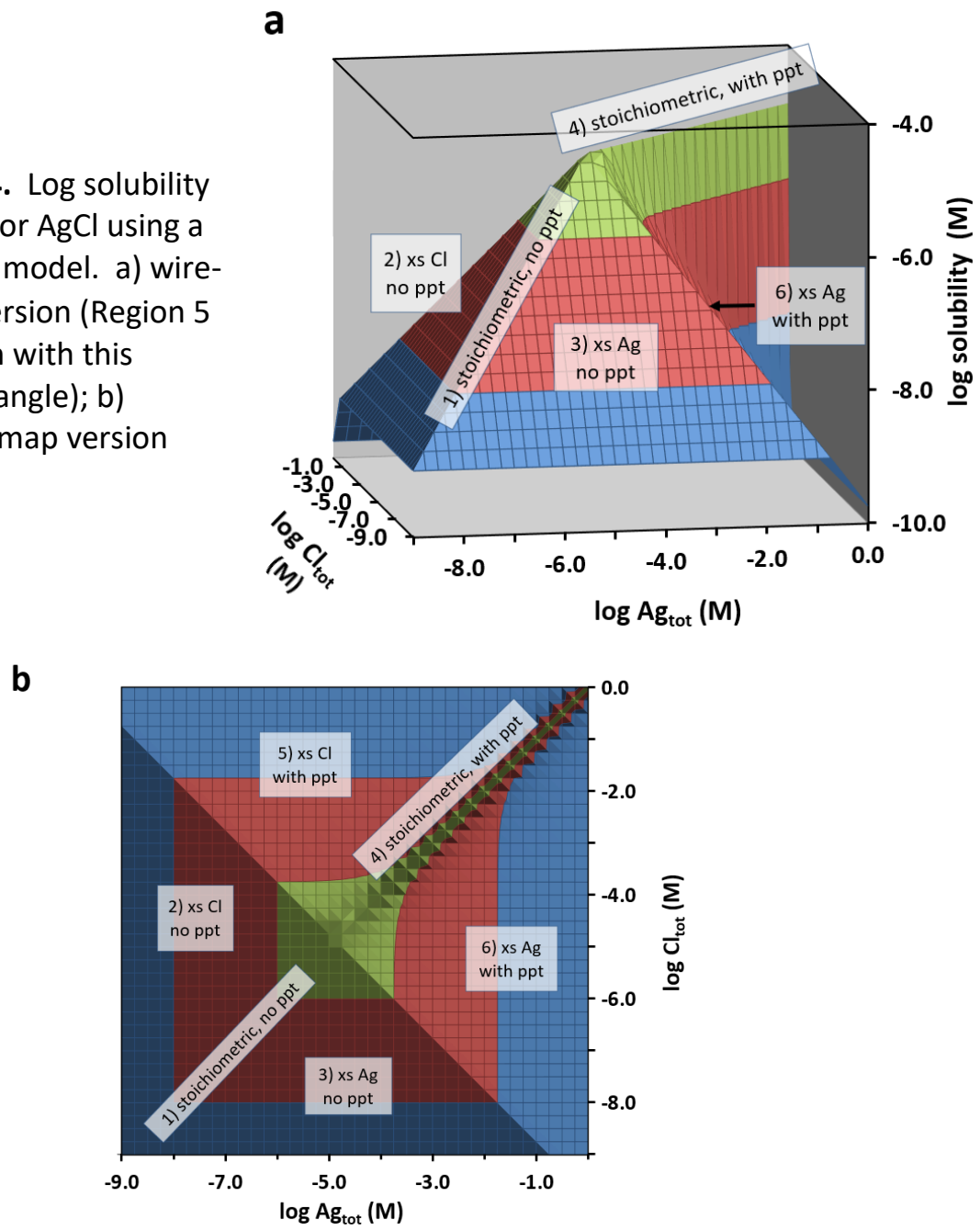

Figure 4.1-4. Log solubility surface for AgCl using a $\mathcal{K}_{sp}$-only model. a) wire-frame version (Region 5 is hidden with this viewing angle); b) contour map version

The solubility composition grid approach generates a prominent ridge along the stoichiometric diagonal. Before the saturation boundary is encountered (Region 1), the stoichiometric diagonal creates an edge where two pyramid faces meet. It climbs at a steady angle until the pyramid's peak is reached. After the saturation boundary (Region 4), the ridge flattens out into a very narrow "spine" that extends to the grid boundary. In pure water, no matter how much AgCl is added, there is a fixed solubility at saturation. Any additional solid, if added, will

just accumulate at the bottom of the container. The solubility of AgCl along the Region 4 maximum solubility ridge follows the familiar formula for a 1:1 salt[4], *i.e.*, solubility = $\mathcal{K}_{sp}^{0.5}$. An artifact of the Excel routine that draws contour maps makes the spine look as if it has triangular struts. Finer grid point increments would continue to shrink the struts to insignificance.

In Region 2, the unsaturated zone with excess Cl^-, the solubility climbs steadily in direct proportion to how much AgCl is added to a solution already containing some Cl^- ion, such as a solution of NaCl. Because the AgCl all dissolves, there is no dependency on the Cl_{tot} value and the surface contours run parallel to the log Cl_{tot} axis. A complimentary behavior is seen in Region 3 for excess Ag^+ conditions.

Region 5 corresponds to situations in which there is excess Cl but some AgCl precipitate is present. This region is not visible in the wire-frame viewing. As can be inferred from the contour map version, Region 5 creates the hidden, back face of the pyramid. The higher the log Cl_{tot} value (moving upward on the grid), the lower the solubility. This the common ion effect, a manifestation of Le Chatelier's principle. The Cl^- ion already present in the solution blocks the ability of Cl^- ions in the crystal lattice from leaving. Any upward grid movement in excess Cl moves down the pyramid face.

Once again, a complimentary behavior is exhibited in Region 6 where there is excess Ag^+ in the presence of some AgCl(*s*) precipitate. This region is barely visible on the wire-frame viewing angle. The viewer is essentially seeing it in profile from the side. It is most perceptible as it curves into the stoichiometric spine at its far edge. If one is moving to the right in the log Ag_{tot} direction, the solubility of AgCl declines. Here it is the extra Ag^+ in solution that is interfering with Ag^+ ion leaving the crystal lattice.

Before leaving the $\mathcal{K}_{sp}$-only model for the AgCl system, it is worth noting that the solubility topos only display what is in solution. They ignore the bulk of the Ag and Cl under saturated conditions that are sitting at the bottom of the container as a solid precipitate. The best way to examine this aspect of the system is to study a segment of the stoichiometric ridge in Region 4. In the next figure, we switch here to a linear composition grid in place of the logarithmic one.

This will help demonstrate the linear relationship between the amount of precipitate and the amount of common ion to either side of the ridge.

Consider an experiment employing the continuous variations strategy.[4] For this approach, a series of solutions is made with the amount of cation and anion systematically stepped in opposite directions. If the total amount of combined solution is kept at 10 mL, for example, Tube 1 would contain 0 mL of cation and 10 mL of anion. Tube 2 would hold 1 mL of cation and 9 mL of anion. Advancing this pattern would have Tube 3 with 2 mL of cation and 8 mL of anion. The series would end with Tube 11 containing 10 mL of cation and 0 mL of anion. We have simulated this situation for the AgCl system and stock solutions of 0.01 M Ag^+ and 0.01 M Cl^-. The linear grid coordinates for each tube are superimposed on the precipitate topo surfaces in Figure 4.1-5. The amount of precipitate is expressed as the molarity it would establish were it in solution.

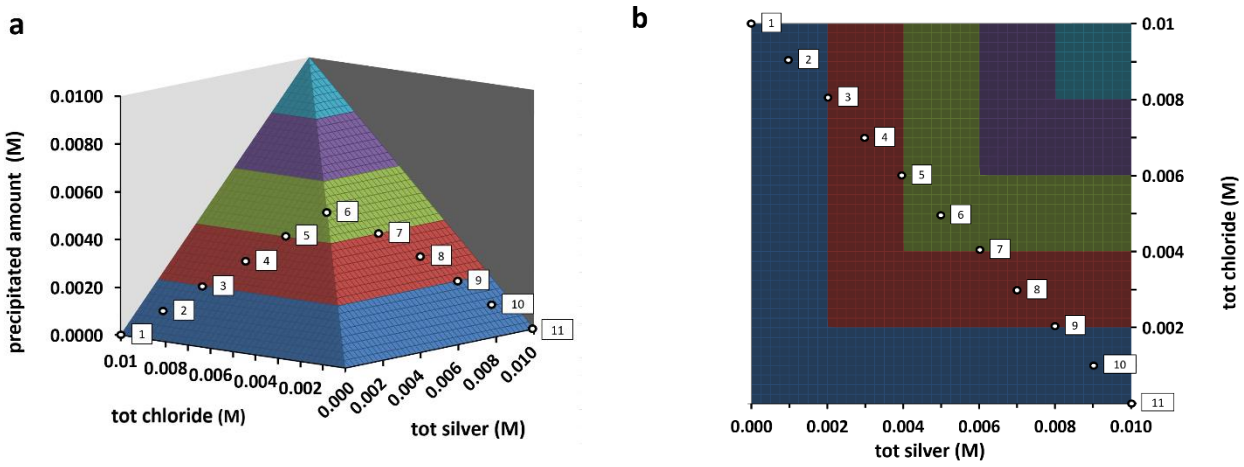

Figure 4.1-5. Precipitate topos for AgCl with continuous variations points noted for a 0.01 M tube series. a) wire-frame; b) contour map.

If the quantity of precipitate is followed over the entire series, the direct relationship between the amount of precipitate and the amount of common ion can be seen (Table 4.1-2 and Figure 4.1-6). In Tubes 1 through 5, there is excess chloride. The excess diminishes with each subsequent tube until there is an exact stoichiometric mix at Tube 6. The maximum amount of precipitate is observed here, a nice demonstration of its 1:1 stoichiometry. Beyond Tube 6, the amount of excess silver ion increases until there is no chloride left to precipitate by Tube 11.

Table 4.2-2. Continuous variation design for AgCl precipitate

Tube number	mL of Ag^+	mL of Cl^-	Relative ppt height
1	0	10	0
2	1	9	1
3	2	8	2
4	3	7	3
5	4	6	4
6	5	5	5
7	6	4	4
8	7	3	3
9	8	2	2
10	9	1	1
11	10	0	0

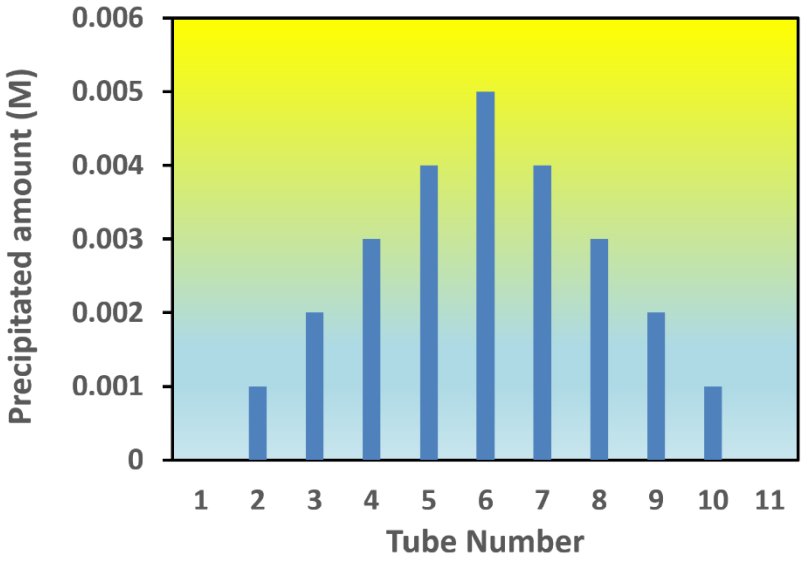

Figure 4.1-6. Precipitated amounts by tube number in the 0.01 M AgCl system.

4.1.4 Beyond the $\mathcal{K}_{sp}$-only Model

The shortcomings of a simple $\mathcal{K}_{sp}$-only interpretation of the aqueous chemistry of AgCl can be highlighted by including model situations in which ion pairing, neutral complexes, higher chloro-complexes, hydroxyl complexes and polynuclear species are present. Here is a list of ever-increasing complexity in solubility systems.

Case 1: The simplistic $\mathcal{K}_{sp}$-only model (already presented) in which dissolved species are limited to just Ag^+ and Cl^-

Case 2: Inclusion of a neutral complex/ion pair, $AgCl^0(aq)$

Case 3: Inclusion of higher, negatively-charged, chloro-complexes and/or hydrolytic silver hydroxyl species - $AgCl_2^-$, $AgCl_3^{2-}$, $AgCl_4^{3-}$, $AgOH^0$, $Ag(OH)_2^-$, etc.

Case 4: Polynuclear complexes – Ag_2Cl^+

The goal of visualizing these more complex systems with 3-D topos is to highlight the importance of having increasingly detailed descriptions of the chemistry that can occur. Presenting these surfaces with the composition grid's wide range of possibilities will provide the knowledge to know under what circumstances the various additional reactions manifest themselves. The Solubility TOPOS program has additional worksheet tabs to include these higher cases. Even though beginning students will not understand the complexities in detail, by simply viewing the surfaces, they could evaluate the impact of omitting various species from a model.

In all higher cases, the solubility of AgCl is enhanced under some conditions because additional forms that incorporate Ag^+ and Cl^- that originated in solid formula units can be present in solution. A new definition of solubility is required for each case and will be included as part of the discussion.

4.1.5 Case 2 – Inclusion of Ion Pairs/Neutral complexes

The first step up in complexity is to recognize that there may be some of the ionic compound present in the solution phase where the cation and anion are still associated with one another. This could be in the form of an ion pair, where two hydrated ions stick together. Or it could also be present as a neutral complex in which the anion is directly attached to the silver ion with no hydration sheaths in between. This is the case for a 1:1 metal-ligand complex. For simplicity, in continuing the silver chloride system, we will represent the collective amount of a 1:1 species present in solution as $AgCl^0$. An equation with its accompanying thermodynamic constant for this interaction is[5]

$$Ag^+ + Cl^- \rightleftharpoons AgCl^0 \qquad \beta_1 = 1.995 \times 10^3 \qquad (4.1\text{-}4)$$

With the presence of an additional species in solution (another formula unit no longer in the crystal lattice of solid AgCl) a new set of solubility definitions is now required (Table 4.1-3).

Table 4.1-3. Solubility definitions for AgCl solubility under Case 2

Composition grid region	Solubility definition
Stoichiometric mix diagonal	$[Ag^+] + [AgCl^0]$
In excess Cl	$[Ag^+] + [AgCl^0]$
In excess Ag	$[Cl^-] + [AgCl^0]$

With the exception of the stoichiometric spine and the tip of the pyramid, inclusion of a neutral species in the AgCl model significantly enhances the solubility at every grid location above the dashed-diagonal saturation boundary of the $\mathcal{K}_{sp}$-only model (see Figure 4.1-4). It affects the appearance of the solubility surface by adding elevated shelves to either side of the stoichiometric spine (Figure 4.1-7). The saturation boundary is no longer a linear feature. It curves toward higher log Cl_{tot} and log Ag_{tot} values. This indicates that the solubility of AgCl has been greatly enhanced by the presence of the neutral species (see labels in Figure 4.1-7b). The saturation boundary from the $\mathcal{K}_{sp}$-only model is shown in the figures as a dashed white line. It does not correlate with pyramid edges except at the upper peak. Extrapolation of the dashed line to its intersection with the contour map's top and right boundaries (where log Cl_{tot} and log Ag_{tot} are 1 M, respectively) corresponds to $p\mathcal{K}_{sp} = 9.745$. With the $AgCl^0$ added in Case 2, the saturation boundary extends beyond the dashed line along the map's top and right edges until about -6.4. Thus, under these conditions, AgCl has increased in solubility by a factor of about $10^{(9.745-6.4)} = 10^{3.345} \approx 2200$. The presence of the neutral species allows the Region 2 and 3 faces of the pyramid to continue their planar slopes to higher levels. The face regions above the dashed white line represent the enhanced solubility that is created by the $AgCl^0$ species being considered.

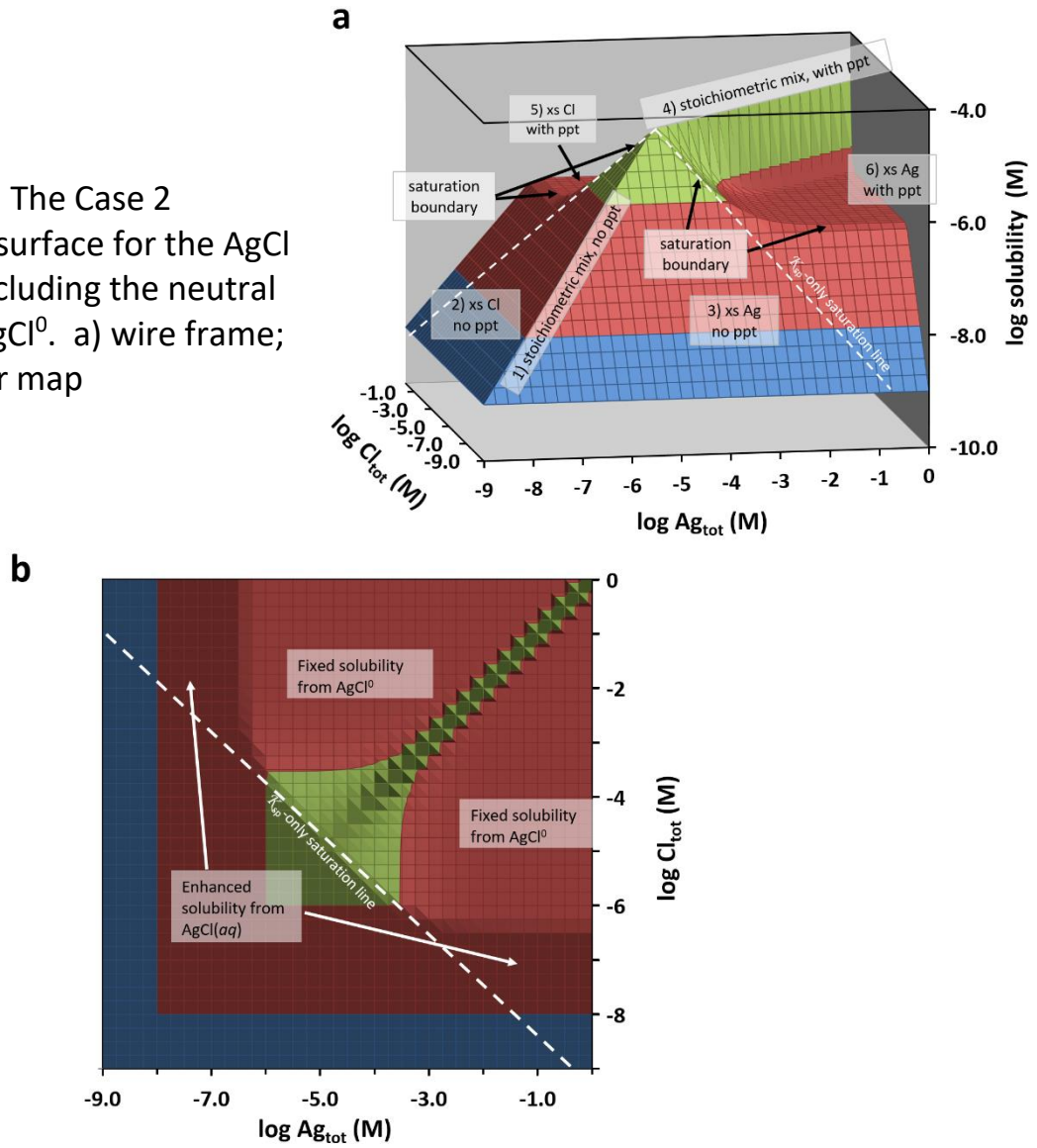

Figure 4.1-7. The Case 2 solubility surface for the AgCl system including the neutral species $AgCl^0$. a) wire frame; b) contour map

Once the saturation boundary has been exceeded, solubility is dominated by the $AgCl^0$ term. It creates a pair of symmetric, broad shelves in Regions 5 and 6 (arrows in Figure 4.1-7b). The presence of these plateaus can be understood by combining the $\mathcal{K}_{sp}$ and β_1 expressions. Under saturated conditions, the $\mathcal{K}_{sp}$ indicates

$$\mathcal{K}_{sp} = [Ag^+][Cl^-] = 1.8 \times 10^{-10} \qquad (4.1\text{-}5)$$

This can be substituted into the expression for β_1

$$\beta_1 = \frac{[AgCl^0]}{[Ag^+][Cl^-]} = 1.995 \times 10^3$$

$$= \frac{[AgCl^0]}{\mathcal{K}_{sp}} = \frac{[AgCl^0]}{1.8 \times 10^{-10}} = 1.995 \times 10^3 \qquad (4.1\text{-}6)$$

Solving eq 4.1-6 for $[AgCl^0]$ yields

$$[AgCl^0] = \beta_1 \mathcal{K}_{sp} = (1.995 \times 10^3)(1.8 \times 10^{-10}) = 3.6 \times 10^{-7} M \qquad (4.1\text{-}7)$$

Thus, eq 4.1-7 reveals that $[AgCl^0]$ is a **constant** under saturated conditions. In other words, not only is the solution saturated with AgCl(*s*), but it is also saturated with respect to $AgCl^0$. Because $[AgCl^0]$ is so much larger than $[Cl^-]$ in Region 5 and $[Ag^+]$ in Region 6, it dominates the solubility contributions and creates the dramatic shelf feature of the solubility topo. For example, on the plateau at grid point (-1.0,0.0) in Region 5, $[Ag^+] = 2.00 \times 10^{-10}$ M while $[AgCl^0] = 3.6 \times 10^{-7}$ M. The ion pair/neutral complex species is 1800 times larger than free Ag^+ ion. Similarly, at (0.0,-1.0) in Region 6, the symmetric aspect of the surface indicates that $[Cl^-] = 2.00 \times 10^{-10}$ while $[AgCl^0]$ is the same **constant** 3.6×10^{-7} M.

Even with the neutral species included, the maximum solubility for AgCl(*s*) remains along the stoichiometric spine. The grid points on this path have no competing common ions to suppress dissolution.

4.1.6 Case 3 for AgCl – Inclusion of Higher Chloro-Complexes

An additional solubility enhancement is seen if chloro-complexes with stoichiometries larger than 1:1 are incorporated into the model. Butler, in his Ionic Equilibrium book[2], includes a set of complexation constants for the higher silver chloride complexes in the system:

$$Ag^+ + Cl^- \rightleftharpoons AgCl^0 \qquad \beta_1 = 10^{3.30} = 1.995 \times 10^3 \qquad (4.1\text{-}8)$$

$$Ag^+ + 2\,Cl^- \rightleftharpoons AgCl_2^- \qquad \beta_2 = 10^{4.72} = 5.248 \times 10^4 \qquad (4.1\text{-}9)$$

$$Ag^+ + 3\,Cl^- \rightleftharpoons AgCl_3^{2-} \qquad \beta_3 = 10^{5.04} = 1.096 \times 10^5 \qquad (4.1\text{-}10)$$

$$Ag^+ + 4\ Cl^- \rightleftharpoons AgCl_4^{3-} \qquad \beta_4 = 10^{5.90} = 7.943 \times 10^5 \qquad (4.1\text{-}11)$$

Once again, a new set of solubility definitions is required for Case 3. The definitions simply add the concentrations of the higher stoichiometry complexes to the list (Table 4.1-4). Note that stoichiometric multipliers were added to the definition under excess Ag conditions. The only way a Cl can appear in solution is if an AgCl formula unit dissolved. Thus, the multipliers on the higher stoichiometries.

Table 4.1-4. Solubility definitions for AgCl solubility under Case 3

Composition grid region	Solubility definition
Stoichiometric mix diagonal	$[Ag^+] + [AgCl^0] + [AgCl_2^-] + [AgCl_3^{2-}] + [AgCl_4^{3-}]$
In excess Cl	$[Ag^+] + [AgCl^0] + [AgCl_2^-] + [AgCl_3^{2-}] + [AgCl_4^{3-}]$
In excess Ag	$[Cl^-] + [AgCl^0] + 2[AgCl_2^-] + 3[AgCl_3^{2-}] + 4[AgCl_4^{3-}]$

With the added aqueous chloro-complex forms, the solubility of AgCl will increase significantly under the excess chlorine conditions of Region 5 (Figure 4.1-8). The enhanced solubility manifests itself as the upsweeping ramp at the back of Region 5 when the wire-frame surface is seen from this viewing angle. This specific ramp is labelled in Figure 4.1-8b. As predicted by Le Chatelier's principle, the extra chloride ion will strongly shift the equilibria in eq 4.1-8 through 4.1-11 to the right.

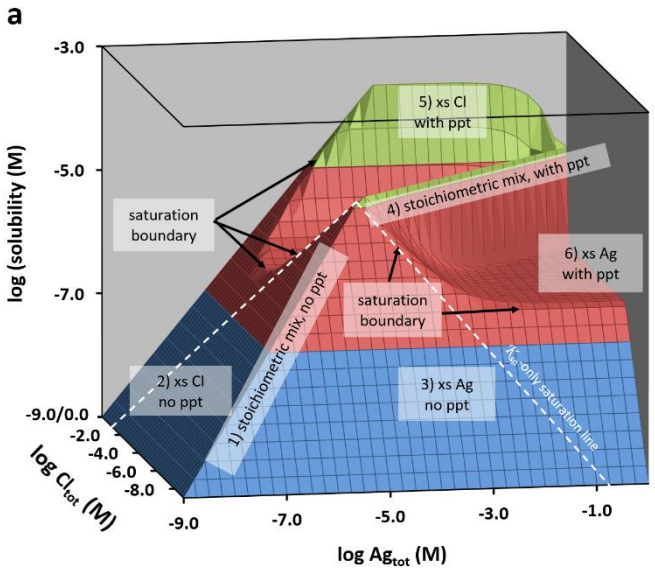

Figure 4.1-8. The Case 3 solubility surface for the AgCl system including higher chloro-complex stoichiometries. a) wire frame; b) contour map (next page)

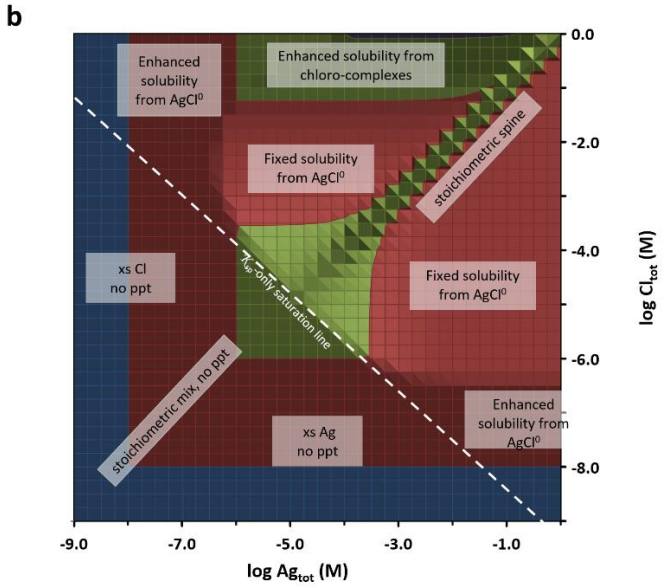

In Region 5, excess Cl with precipitate present, the saturation boundary follows the edge of the rising ramp in Figure 4.1-8 until near log Ag_{tot} = -3.75. An inspection of the Solubility TOPOS data arrays for each species that contributes to the solubility in Region 5 reveals the following species distributions at the grid point (-1.0, 0.0): $[Ag^+] = 2.001 \times 10^{-10}$ M, $[AgCl^0] = 3.600 \times 10^{-7}$ M, $[AgCl_2^-] = 8.502 \times 10^{-6}$ M, $[AgCl_3^{2-}] = 1.598 \times 10^{-5}$ M, $[AgCl_4^{3-}] = 1.041 \times 10^{-4}$ M. Clearly, the chloro-complexes are dominating the distribution of silver in the aqueous portion of the system under these conditions. The concentration of the 1:4 complex alone is 520,000 times larger than the free metal Ag^+ ion. This points out just how poor the Case 1 ($\mathcal{K}_{sp}$-only) model is at describing what goes on in solution. The solubility in the Case 3 complexation model is 1.289×10^{-4} M compared to a solubility for the same grid point in the $\mathcal{K}_{sp}$-only model of 2.00×10^{-10} M. The Case 3 topo maximum is 12.5 times higher than the Case 1 topo maximum. In fact, the enhanced solubility of silver halide salts through complexing conditions was used in the past to recover the valuable silver from photographic developing and X-ray film sludge. [6]

Region 6, excess Ag with precipitate present, shows a prominent horizontal shelf feature. It is worth mentioning that a flat spot on topo surfaces represents a "buffer" situation. On the pH topos of Chapter 1.1, the plateaus corresponded to the classical acid/base buffer phenomenon. In Chapter 2.1, the plateaus represent metal ion buffering. By analogy, the plateau in Figure 4.1-8 could be

termed “solubility buffering”. The addition of more Ag or Cl does not affect the solubility of the system over this portion of the composition grid.

A better understanding of how complexation enhances the solubility of AgCl can be seen by looking at species distribution diagrams of solubility surface slices. Solubility TOPOS contains a tab that permits the user to see individual slices of the surface parallel to the log Cl_{tot} axis. This was chosen because it includes Regions 2 or 5 where complexation reactions begin to become important. Complexation is very limited when there is excess Ag. Accompanying the solubility slice are the distribution curves for all silver species. These are expressed as gammas where γ_0 represents the fraction of silver in the Ag^+ form, γ_1 is the fraction of $AgCl^0$, γ_2 is the fraction of $AgCl_2$, etc. The solubility slice and distribution curves for log Ag_{tot} = 10^{-4} M is shown as Figure 4.1-9. A point spacing of 0.1 log units helps increase curve details.

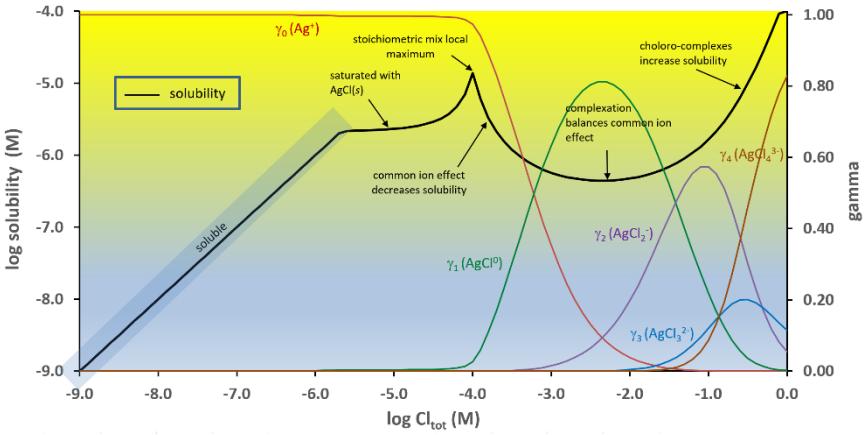

Figure 4.1-9. Solubility for the log Ag_{tot} = 0.0001 M slice of the AgCl Case 3 surface. Superimposed are the γ-curves for all silver-containing species.

The solubility curve is quite complex with different regions in which various effects are manifest. At the left edge of the figure is a linear ramp that essentially varies directly with the log Cl_{tot} value. This is because the saturation boundary has not yet been reached. Everything stays in solution. Thus, solubility = log Cl_{tot}. As there is an excess of Ag for this portion of the slice, there is little chloride to make any higher stoichiometry complexes. Almost all of the silver is present in the uncomplexed Ag^+ form. Over this entire range γ_0 is for all intents 1.00. The other γ’s are essentially zero for this range.

The saturation boundary is encountered when the trial ion product (TIP), $[Ag^+][Cl^-]$, equals the $\mathcal{K}_{sp}$ of AgCl at 1.8 x 10^{-10} M. The first grid point beyond the

saturation boundary occurs when log Cl_{tot} is -5.6. At this location $[Ag^+]$ = 9.930 x 10^{-5} M and $[Cl^-]$ = 1.813 x 10^{-6} M. There is very little precipitate yet, only 3.392 x 10^{-7} M missing from solution. But the solution is saturated with respect to AgCl(*s*). It is also saturated with respect to the $AgCl^0$ neutral complex at 3.600 x 10^{-7} M. This concentration is two orders of magnitude below that for $[Ag^+]$, so γ_0 is still close to 1 at 0.996.

As the solubility curve approaches the stoichiometric mix value of log Ag_{tot} = log Cl_{tot} = 1 x 10^{-4} M, the curve rises ever more steeply to a local maximum at the stoichiometric ridge. The solubility keeps increasing as the ridge is approached because there is less and less of the common Ag^+ ion present. This slope is not linear due to the growing amount of $AgCl^0$ that begins to form. At the grid point just before the stoichiometric mix ridge (log Cl_{tot} = -4.1), the neutral complex is now 1.3% of the silver in solution. The precipitation process has also removed 10.3% of the total silver.

A local solubility maximum occurs near the stoichiometric mix point. Because of the higher chloro-complexation side reactions, this does not land exactly on the grid point. It does not, however, miss by much. The Ag^+ and Cl^- ion concentrations only differ in their sixth significant figures. There is still no excess Cl^- to participate in forming the higher stoichiometries. The maximum exists because the common ion effect is minimized here. Neither component ion is in excess.

Beyond the stoichiometric ridge, there is a rapid decline in solubility caused by an ever-growing level of the common Cl^- ion that forces AgCl(*s*) to precipitate. At the same time, however, the quantity of $AgCl^0$ begins to steadily increase. There is even a bit of $AgCl_2^-$ starting to appear around log Cl_{tot} = -3.4. The solubility stops decreasing when the growing complexation exactly counterbalances the common ion effect. The common ion that is being added is simultaneously being removed by the complexation process. Even though more Cl^- is available, it is tied up in chloro-complexes, not being precipitated out. The balance point occurs when log Ag_{tot} = -2.4. Here, γ_1 is 0.812; the aqueous system is dominated by $AgCl^0$. The Ag^+ is declining with a γ_0 of 0.102. $AgCl_2^-$ is starting to take off with its γ_2 at 0.0827.

Once the common ion balance point is surpassed, complexation really gains momentum. The higher stoichiometries grow in prominence. First the 1:2 and then the 1:4 complex dominate the aqueous species. The 1:3 complex never dominates in this slice. At the final point, γ_4 is 0.829, γ_3 is 0.114 and γ_2 is 0.0548 such that 99.8% of the aqueous species are the three higher complexes. It is interesting to note that this final point has traversed back into the "soluble" region of the surface. The TIP is 1.044×10^{-10}, slightly below the $\mathcal{K}_{sp}$ of 1.8×10^{-10}.

4.1.7 Solubility Surfaces for Non-1:1 Stoichiometries

Sparingly soluble salts with stoichiometries beyond a 1:1 ratio show similar solubility topos, but they will have asymmetric pyramids. As an illustration, consider Case 1 (the $\mathcal{K}_{sp}$-only model) for lead(II) iodide, PbI_2, that has a $\mathcal{K}_{sp}$ of 7.9×10^{-9}. Solubility definitions must be revised slightly for this 1:2 stoichiometry (Table 4.1-5). Because two I^- ions are released for each formula unit that dissolves, the solubility in the stoichiometric mix or excess Pb^{2+} must be defined as half of the I^- concentration.

Table 4.1-5. Solubility definitions for PbI_2 solubility under Case 1

Composition grid region	Solubility definition
Stoichiometric mix	$[Pb^{2+}]$ or $0.5[I^-]$
In excess I	$[Pb^{2+}]$
In excess Pb	$0.5[I^-]$

A complication in visualizing the solubility topos is encountered for the 1:2 stoichiometry because the regular-spaced grid points used to generate the surface misses the stoichiometric spine completely (Figure 4.1-10). The dotted line corresponding to the stoichiometric ridge does not hit any grid points (the intersections of the horizontal and vertical lines) anomalies across the entire topo. This is evident, for example, in Region 4 at the upper edge of the grid. The ridge hits the edge when $Pb_{tot} = 0.5$ M and $I_{tot} = 1.0$ M. This corresponds to (log Pb_{tot}, log I_{tot})-grid coordinates of (-0.301, 0.0). The grid points are at increments of 0.25 log units, so the exact spine coordinates are missed. The spine lands between the (-0.25, 0.0) and (-0.50, 0.0) grid points.

Figure 4.1-10. Solubility assignment regions for the PbI_2 system under Case 1 – $\mathcal{K}_{sp}$ only. Note that the stoichiometric ratio path for a 1:2 salt misses grid point intersections at every occasion.

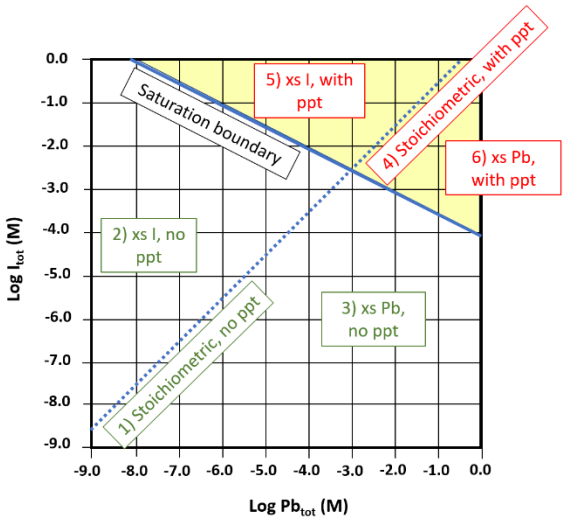

The $\mathcal{K}_{sp}$-only solubility topos for the PbI_2 system are shown in Figure 4.1-11. While the overall surface still retains a pyramidal shape, its peak is offset toward higher log I_{tot} values. The Region 2 and 3 faces, that represent unsaturated conditions when no solid is present, are inclined at 45° as before. The face for Region 5 (where there is excess iodine beyond the saturation boundary), however, is tipped more steeply at 60°. The face for Region 6 (excess Pb^{2+} in saturated solutions) is more shallowly sloped at 30°. In the contour map of Figure 4.1-11b, Region 5 displays narrower colored bands because of the steeper slope and Region 6 displays correspondingly broader colored bands indicating the shallower slope.

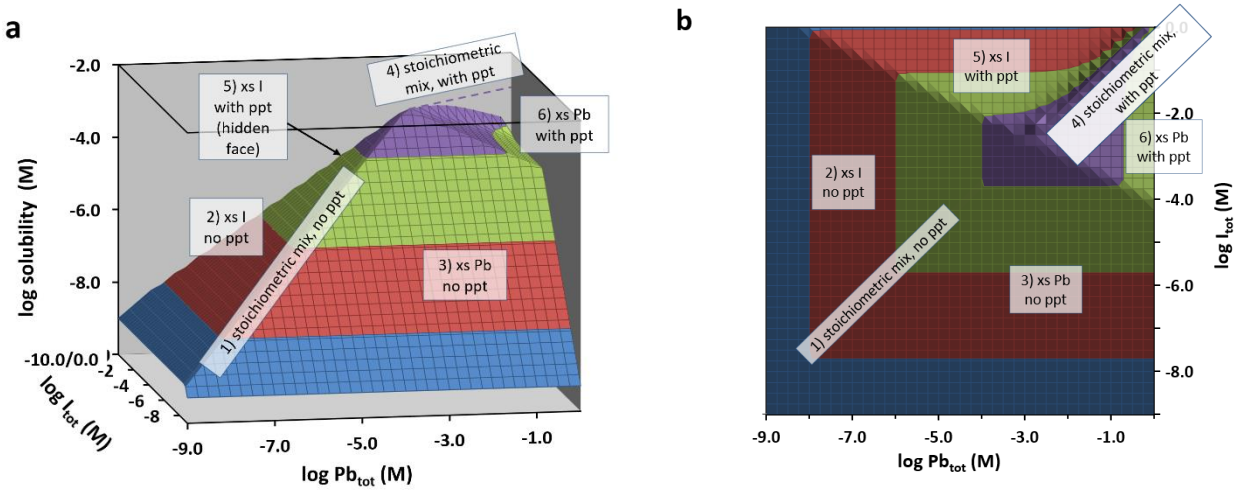

Figure 4.1-11. Log solubility surfaces for the $\mathcal{K}_{sp}$-only model (Case 1) of PbI_2. a) wire-frame; b) contour map

The small peak at the top of the pyramid, where the saturation boundary intersects the stoichiometric spine, is not quite the maximum. The maximum is missed by our grid-point spacing. Once the saturation boundary is encountered, the solubility is constant for the remainder of the spine's run, not a peak with a row of diminishing values following the spine's path. The highest grid point on the displayed solubility surface occurs when log Pb_{tot} is at -2.75 and log I_{tot} is -2.5. At this location, it shows a log solubility value of -2.92, equivalent to 1.19 x 10^{-3} M. Had the actual stoichiometric ridge point been computed, the highest resulting log solubility would be -2.901, equivalent to 1.25 x 10^{-3} M, slightly higher. This maximum value would then continue as a sharp ridge (see dotted purple line in Figure 4.1-11a) all the way to the upper surface edge at (-.301, 0.0), similar to the stoichiometric ridge for the AgCl system seen in Figure 4.1-4.

4.1.8 Cases 2 and 3 for PbI_2 – Inclusion of Aqueous Iodo-Complexes

Lead iodide can serve to illustrate the solubility enhancement from higher stoichiometry complexes for a solid with a 1:2 stoichiometry. With the Pb^{2+}/I^- system, complexes of up to 1:4 are possible.

$$Pb^{2+} + I^- \rightleftharpoons PbI^+ \qquad \beta_1 = 10^{2.00} = 1.0 \times 10^2 \qquad (4.1\text{-}12)$$

$$Pb^{2+} + 2\,I^- \rightleftharpoons PbI_2^0 \qquad \beta_2 = 10^{3.15} = 1.4 \times 10^3 \qquad (4.1\text{-}13)$$

$$Pb^{2+} + 3\,I^- \rightleftharpoons PbI_3^- \qquad \beta_3 = 10^{3.92} = 8.3 \times 10^3 \qquad (4.1\text{-}14)$$

$$Pb^{2+} + 4\,I^- \rightleftharpoons PbI_4^{-2} \qquad \beta_4 = 10^{4.48} = 3.0 \times 10^4 \qquad (4.1\text{-}15)$$

As given earlier, the $\mathcal{K}_{sp}$ for $PbI_2(s)$ is 7.9 x 10^{-9}.

It is again necessary to revisit the definitions for solubility in this system to take account of the 1:2 stoichiometric factor. These new definitions recognize that one formula unit of dissolved PbI_2 places two iodine atoms in some form in the aqueous phase (Table 4.1-6).

Table 4.1-6. Solubility definitions for PbI_2 solubility under Case 2 and 3

Composition grid region	Solubility definition
Stoichiometric mix	$[Pb^{2+}] + [PbI^+] + [PbI_2^0] + [PbI_3^-] + [PbI_4^{2-}]$
In excess I	$[Pb^{2+}] + [PbI^+] + [PbI_2^0] + [PbI_3^-] + [PbI_4^{2-}]$
In excess Pb	$0.5([I^-] + [PbI^+] + 2[PbI_2^0] + 3[PbI_3^-] + 4[PbI_4^{2-}])$

Case 2 for the PbI_2 solubility system includes only the neutral species, designated here as PbI_2^0. The solubility definitions would exclude the other iodo-complexes in the Table 4.1-6 definitions. The solubility surfaces for Case 2 appears as Figure 4.1-12. Because the PbI_2 system is more soluble than the AgCl system, the precipitate region is smaller in extent on these plots. The main differences between the Case 1 surface ($\mathcal{K}_{sp}$-only) and the Case 2 surface (a neutral aqueous iodo-complex) are emphasized with the text box label on the contour map version (Figure 4.1-12b). There is an enhancement of the Region 2 (no-precipitate in excess Pb) because the PbI_2^0 diverts some of the excess Pb^{2+} common ion into a soluble form. Once the saturation boundary has been reached at log Pb_{tot} = -4.75, there is a plateau indicating that solubility is now dominated by the PbI_2^0 term. At saturation, in the presence of $PbI_2(s)$, the concentration of PbI_2^0 is fixed at a value of 1.106 x 10^{-5} M.

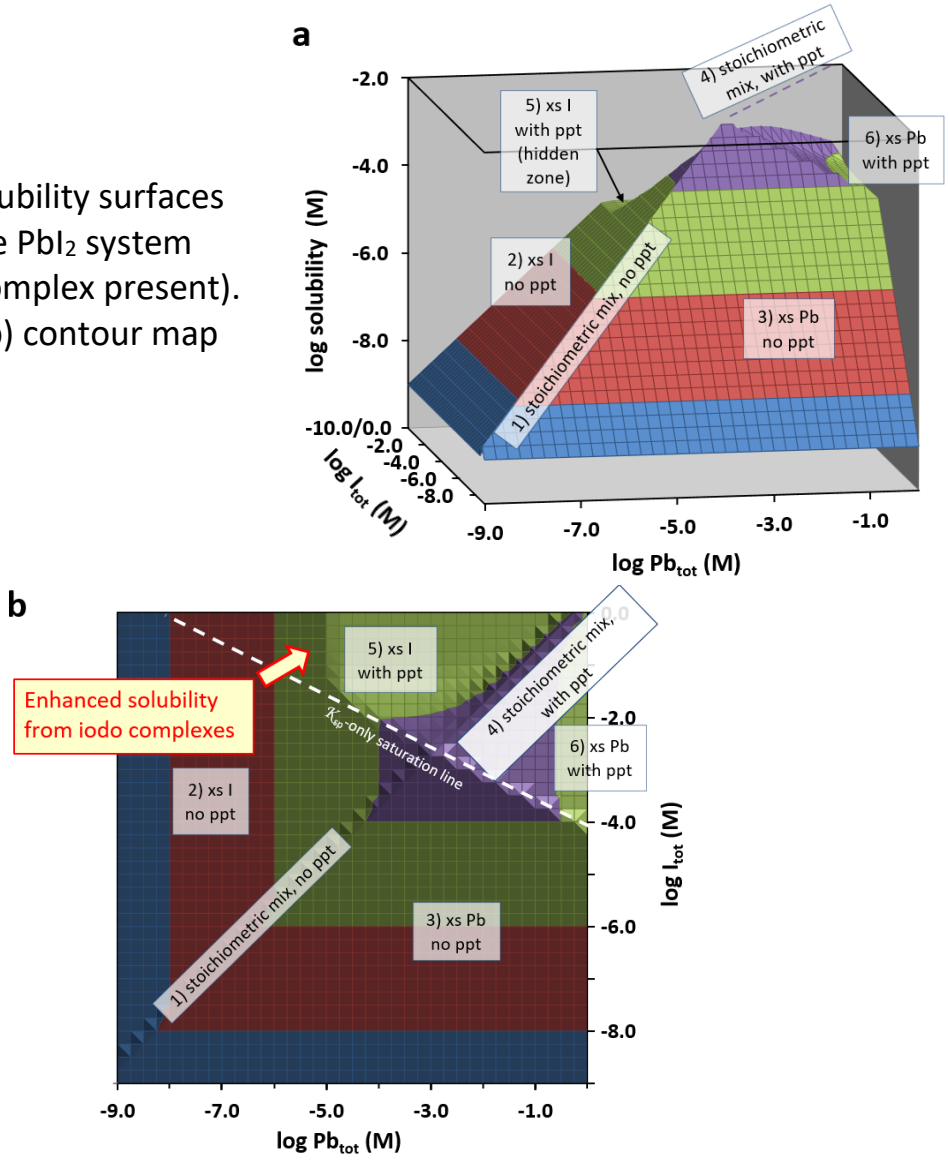

Figure 4.1-12. Solubility surfaces for Case 2 of the PbI_2 system (neutral iodo-complex present). a) wire-frame; b) contour map

Case 3 for the PbI_2 system includes four iodo-complexes that can form with Pb^{2+}. Compared to Case 2, there are two clear differences that can be seen for the Case 3 solubility surface (Figure 4.1-13). First, there is a ramp in Region 5 sweeping upward as I_{tot} increases. This is due to the presence of higher iodo-complexes forming, especially PbI_4^{2-} along the log I_{tot} = 0 (*i.e.*, 1.0 M) back edge. This is analogous to the ramp in the Case 3 plot for AgCl seen in Figure 4.1-8 and expanded in Figure 4.1-9. Second, and more interesting, the top of the solubility pyramid continues in an upsloping wedge not observed in the 1:1 AgCl system.

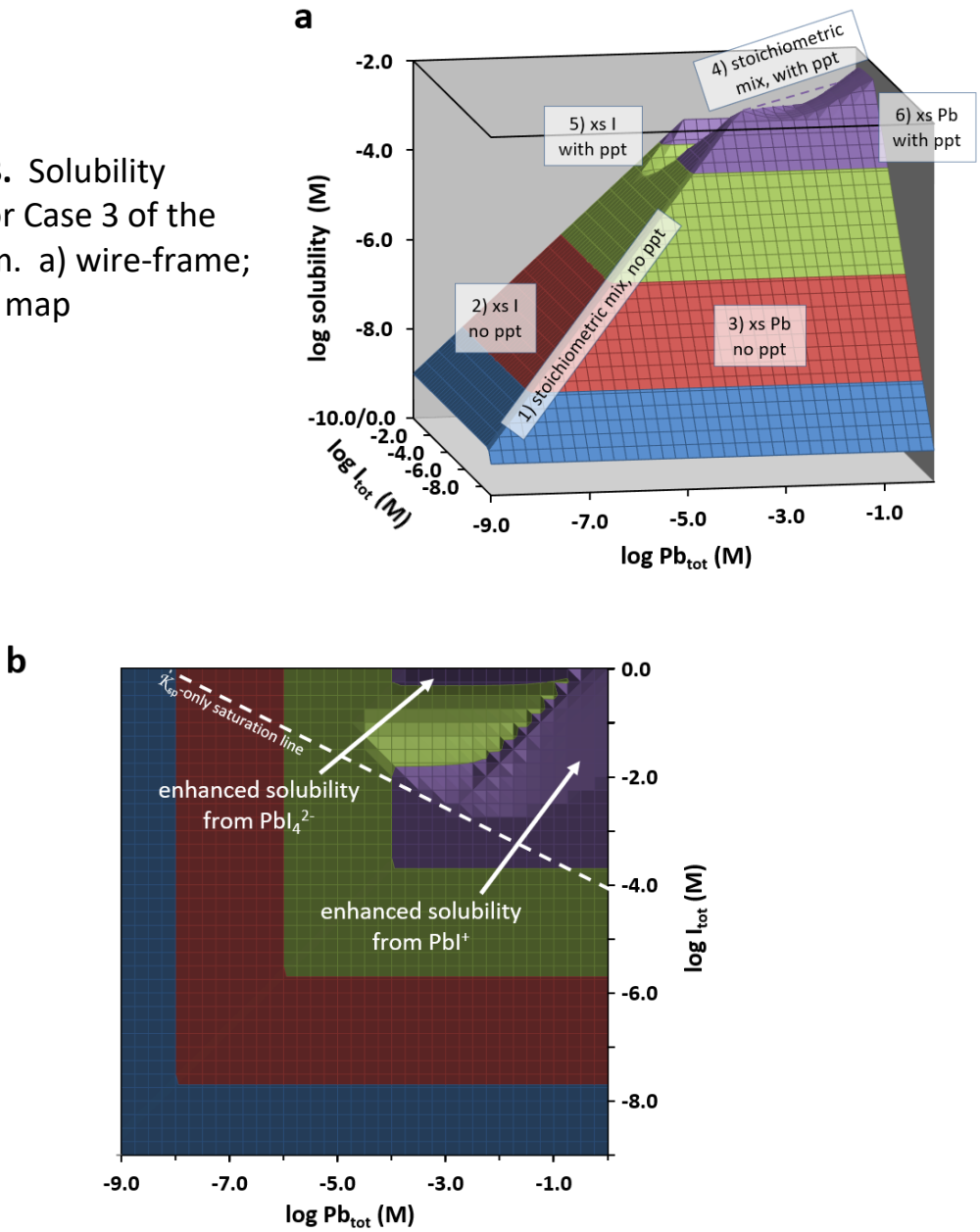

Figure 4.1-13. Solubility surfaces for Case 3 of the PbI_2 system. a) wire-frame; b) contour map

The upsloping wedge portion of the surface continues to higher levels than the tip of the previously-established pyramidal portion of the surface. The maximum solubility exhibited in this system occurs when log Ag_{tot} = 0 (*i.e.*, 1 M) and log I_{tot} = -2.0 (*i.e.*, 0.01 M). It is the contribution of significant amounts of PbI^+ complex that is responsible for the enhanced solubility here. The valley that is hidden behind the upsloping wedge on the wire-frame surface can be seen by changing the viewing angle (Figure 4.1-14). In the log I_{tot} direction, the valley is caused by the common ion effect reducing solubility until formation of higher complexes overtakes that. In the log Pb_{tot} direction, it eventually hits the stoichiometric mix ridge.

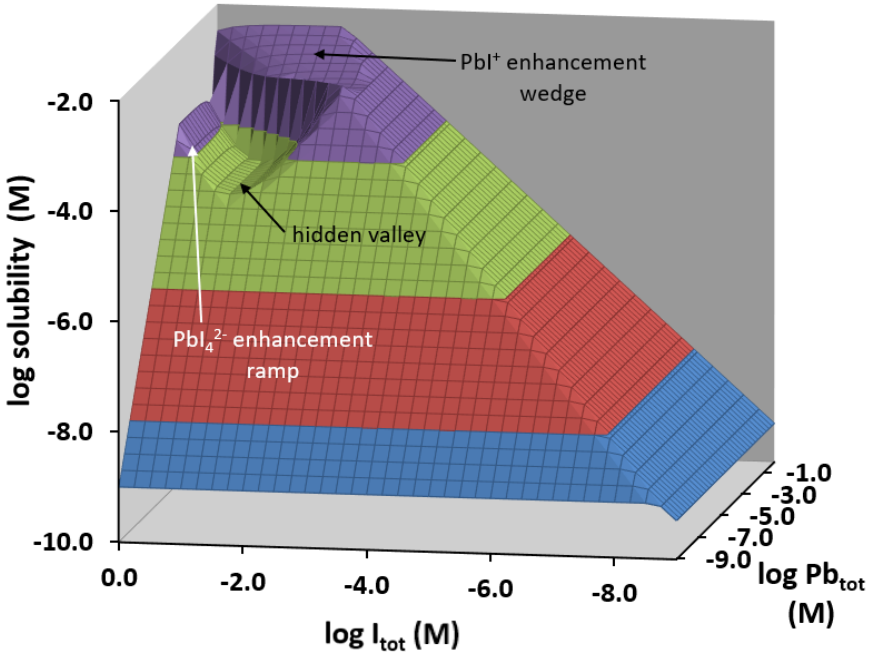

Figure 4.1-14. The hidden valley on the wire-frame solubility surface for PbI_2 seen from a different viewing angle

Another way to emphasize the dramatic increase in solubility created by the PbI^+ complex is to replot the solubility surface with a linear *z*-scale (Figure 4.1-15). Use of this vertical axis compresses low solubility values but accentuates high solubilities. The solubility enhancement created by PbI^+ in the grid region to the right of the stoichiometric mix line (*i.e.*, excess Pb^{2+}) is seen as a tall pinnacle. The solubility at the surface's maximum (4.48 x 10^{-3} M) is greater by more than a factor of three over the tip of the solubility pyramid feature (1.36 x 10^{-3} M). Given the ranges of the composition grid base, this location for the maximum solubility is a spot that intuition might not have previously suggested, another example of

the new insights that the composition grid approach offers. A second ridge of solubility enhancement appears at the back edge of the surface. This is where higher iodo-complexes such as PbI_4^{2-} become dominant forms as explained earlier.

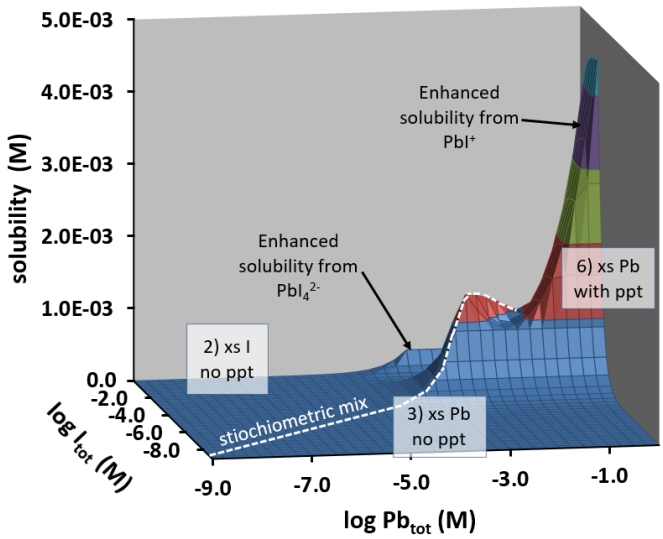

Figure 4.1-15. Solubility in the Pb^{2+}/I^- system with a linear vertical axis

Confirmation that the maximum solubility is driven by $[PbI^+]$ can be seen from the PbI^+ topo (Figure 4.1-16). Note that it possesses the same tall pinnacle in the same portion of the composition grid. Its concentration maximum is TWICE that of the solubility surface because the solubility definition for excess Pb is solubility = $0.5([I^-] + [PbI^+] + 2[PbI_2^0] + 3[PbI_3^-] + 4[PbI_4^{2-}])$ because for each formula unit of PbI_2 that dissolves, two I^- ions become available for complexing with the excess Pb^{2+}.

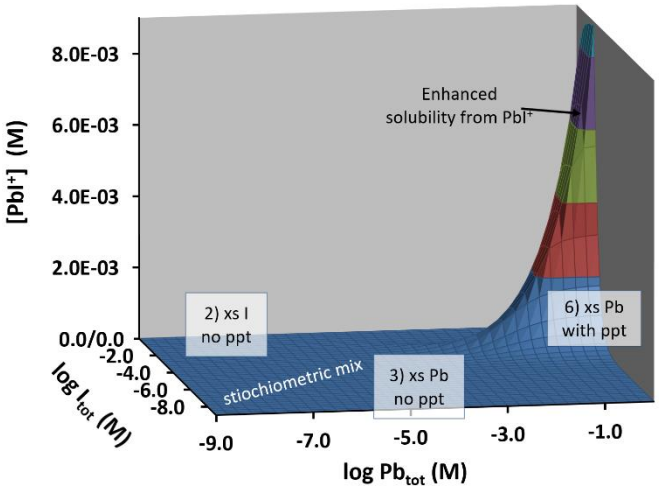

Figure 4.1-16. The PbI^+ topo showing a PbI^+ maximum twice that of the PbI_2 solubility maximum at the same grid point.

4.1.9 Conclusions

A new composition grid approach to describing sparingly soluble salts has been developed, plotting concentration of the metal cation as an x-axis and the concentration of the anion as the y-axis. When the solubility of the salt is plotted as a vertical axis, details of its behavior over a wide range of conditions become easily visualized as topo surfaces. As developed, this chapter reveals shortcomings that are created by the incomplete description of the chemistry included in a computational model. Case 1, the $\mathcal{K}_{sp}$-only version, gives rise to a pyramidal surface that misses inclusion of all soluble complexes in the system for Case 3. The maximum solubility of AgCl for Case 3 is 1.72×10^{-4} M while that for Case 1 was only 1.34×10^{-5}, more than an order of magnitude less. The difference between the two models is visually highlighted using the topo surface approach. While the computations for Case 3 are quite complicated, the use of the Solubility TOPOS program that is part of the supplementary files for this chapter makes it accessible to even beginning students when they are provided with the complex species that should be considered and their accompanying equilibrium constants.

A second aspect of the solubility topos is that they entice the viewer into examining solubility when it incorporates situations other than simply dissolving a solid salt in pure water. Dissolving the solid salt comprises only a diagonal spine of the solubility topos from at or near the front corner to at or near the back corner. All other grid points relate to solubility equilibria that come into play when a common ion is present in the aqueous phase. In both example systems that are detailed in this chapter, the maximum solubility conditions are not found along the diagonal stoichiometric spine. We ourselves are not always able to foresee where the maximum will land until we run the Solubility TOPOS program.

The Solubility TOPOS software is easy to run. Users need only to identify the stoichiometry of the solid precipitate and any complex species they wish to include. A tab on the software contains a number of systems for which relevant formulas and thermodynamic constants have been provided up to a 1:6 complex stoichiometry. Use of Solubility TOPOS is appropriate for introductory courses when they are addressing simple solubility equilibria. The interpretation of many modeling results, however, will require the chemical sophistication of students in junior- or graduate-level courses in analytical chemistry, physical chemistry,

biochemistry and aquatic chemistry. The speed and ease with which new systems can be visualized makes this a powerful tool for simulation studies.

Because Solubility TOPOS is implemented via Microsoft Excel, no new software need be purchased to run it. Run-times are typically a few minutes. Solubility TOPOS can conveniently be used for "on the fly" calculations by an instructor during a live classroom session, although a bit of discussion during the run-time may be necessary. None the less, a query from a student about "What would happen to the solubility if…" can rather quickly be addressed with a new program run.

4.1.10 Supplementary Files

Five downloadable files are included as additional supplements for this chapter:

1. The downloadable Solubility TOPOS software implemented as a Microsoft Excel workbook that includes possible combinations of metal cations and anions from which to form precipitates. Users can supply their own information for systems not included in the compilation.

2. A set of Microsoft PowerPoint slides from which to present a lecture on solubility surfaces. Teaching points are highlighted and illustrated with extensively annotated surfaces on the slides.

3. The "Teaching with Solubility TOPOS" file contains itemized learning objectives, with each objective matched to a range of slides in the PowerPoint file. Also included are suggested Solubility TOPOS workbook activities (homework, prelab, recitation, or peer-led team discussions).

4. A detailed explanation of how the macros generate the solubility value for each point depending on which region of the surface it belongs (*e.g.*, Region 1 – the stochiometric ridge, Region 2 - excess anion with no precipitate, Region 3 – excess metal cation with no precipitate, etc.).

5. A code listing for the solubility calculation macros.

Author Information

Corresponding Author

*E-mail: garon.smith@umontana.edu

ORCID

Garon C. Smith: 0000-0003-0145-8286

Acknowledgments

The authors are grateful to the Department of Chemistry and Biochemistry at the University of Montana for graduate teaching assistantships during the doctoral program of MMH. Patrick MacCarthy, Department of Chemistry and Geochemistry, Colorado School of Mines contributed to early formulation of the solubility composition grid concept.

References

1. Clark, R.W.; Bonicamp, J.M. The $\mathcal{K}_{sp}$- Solubility Conundrum. *J. Chem. Educ. 75(*9*),* **1998***,* 1182-1185*.* https://doi.org/10.1021/ed075p1182
2. Butler, J. N. Ionic Equilibrium: Solubility and pH Calculations, John Willey & Sons, Inc., New York, NY, 1998. ISBN: 978-0-471-58526-8
3. Fritz, J. J. Thermodynamic Properties of Chloro-Complexes of Silver Chloride in Aqueous Solution. *J. Solution Chem.*, **1985**, *14*(12), 865-879. https://doi.org/10.1007/BF00646296
4. Job, P. Formation and Stability of Inorganic Complexes in Solution. *Annales de Chimie*., **1928**, *10*(9), 113–203.
5. Harris, D. *Quantitative Chemical Analysis. 8th Edition*; Freeman: New York, 2010, AP20-AP27. ISBN: 1429218150
6. Silver Recovery from X-Ray Film and Other Film Products? (maratek.com) accessed 12/27/2022.